Monografías de la Real Academia de Ciencias de Zaragoza **34**, 87–104, (2010).

Physics-based Modeling of Fire Spread in Densely-built Urban Area and its Application to Risk Assessment

Keisuke Himoto and Takeyoshi Tanaka

Kyoto University
Gokasho, Uji, Kyoto 611-0011, Japan

Abstract

A fire staring in a densely-built urban area easily spreads to adjacent buildings. Especially, in the case of a large earthquake, in which multiple fires may break out simultaneously, the momentum of fire spread may easily overwhelm the ability of firefighters and cause disastrous damage to the area. It is recently reported that there are substantial area still left in Japan which requires some social intervention for improving safety from fire spread. In this study, fire spread simulations were carried out in order to investigate behavior of fire spread in Kyoto Higashiyama area, one of the representatives of densely-built urban areas in Japan. In the numerical model, urban fire is assumed as an ensemble of multiple building fires, that is, the fire spread is simulated by predicting behaviors of individual building fires under the thermal influence of neighboring building fires. Adopted numerical technique for the prediction of individual building fire behavior is based on the one-layer zone model. Governing equations of mass, energy, and chemical species in component rooms are solved simultaneously, for the development of temperature, concentrations of chemical species, and other properties. As for the building-to-building fire spread, following mechanisms are considered as contributing factors of fire spread: thermal radiation heat transfer from fire-involved buildings; thermal convection by wind-blown fire plumes originated from fire-involved buildings in the upwind; and spotting ignition by dispersed firebrands. With this numerical model, the risk of fire spread in Kyoto Higashiyama area was assessed by the Monte Carlo method. Effectiveness of measures against fire spread was also investigated by comparing results of the risk assessment.

Keywords: Urban fire; Fire Spread; Densely-built Urban Area; Risk Assessment

1 Introduction

When a fire initiates in a densely-built urban area, it easily propagates to adjacent buildings one after another. Especially in the case of large earthquake, when multiple fires break out simultaneously, hazard of the fire spread is likely to overwhelm the ability of fire fighting and cause disastrous damage to the urban area. Such fire involves as many as thousands or even more building fires at a time. The fire followed Kobe Earthquake in 1995 which burnt about 66ha of city area in total is a recent example (Fig. 1).

Figure 1.— Fire followed 1995 Kobe Earthquake [1].

Figure 2 shows a street view of densely-built urban area in Japan. Common problems of such areas regarding fire safety include: (a) narrow streets enabling fire to spread easily from one building to another; (b) streets cluttered with collapsed buildings in an earthquake restricting fire engine to access; (c) shortage of open spaces which serve as fire breaks or evacuation sites; (d) older and less robust wooden houses that easily collapse and burn in an earthquake; (e) a majority of elderly residents with little motivation for rebuilding old housing; and (f) building sites not meeting requirements of the latest Japanese Building Standard Law, restricting the building of new and fire-resistant houses. It is reported that there are 25,000ha of densely-built urban area still left in Japan which requires some sort of fire safety measures to be implemented [2].

The importance of urban reconstruction of densely-built urban areas has not necessarily been underestimated, because fires and other disasters such as earthquakes are common in Japan. One of the reasons behind the lack of urban management is attributed to legislations such as the Building Standard Law and the City Planning Law. They are not authorized to forcibly implement appropriate construction without social consensus on the need for controlled urban reconstruction. Daily life in densely-built urban environments did not necessarily involve under-privileged populations requiring social intervention by

Figure 2.— Street view in a densely-built urban area.

the government. Residents had no imminent concerns encouraging them to reconstruct their environments, except the threat of natural disasters. However, as the occurrence of natural disasters is unpredictable, no one knows whether an earthquake will strike the city tomorrow or 100 years later.

In order to devise an effective measure against urban fires, risk and behavior of fire spread in urban areas need to be evaluated. For this purpose, a physics-based urban fire spread model was developed, in which urban fire is treated as a collection of individual building fires that evolve under the thermal influence from surrounding building fires [3]. The model was verified by comparing the computational results with the past fire event, and reasonable agreement was obtained. In this study, fire spread simulations were carried out in order to investigate behavior of fire spread in Kyoto Higashiyama area, one of the representatives of densely-built urban areas in Japan. The principal advantage of the physics-based modeling is that it enables detailed and rational analysis of fire spread in urban area. Utilizing this feature of the model, the risk of fire spread within the target area was assessed by the Monte Carlo method and effectiveness of fire safety measures was evaluated.

2 Outline of the urban fire spread model

Schematic diagram of the present model is shown in Fig. 3. In the model, spread of fire in urban area is described by simulating the behaviors of individual building fires under the influence of neighboring building fires, as urban fire is nothing but an ensemble of multiple building fires. Thus the model consists of two major sub-models: one that describes fire behaviors inside buildings; and another that describes building-to-building

fire spread.

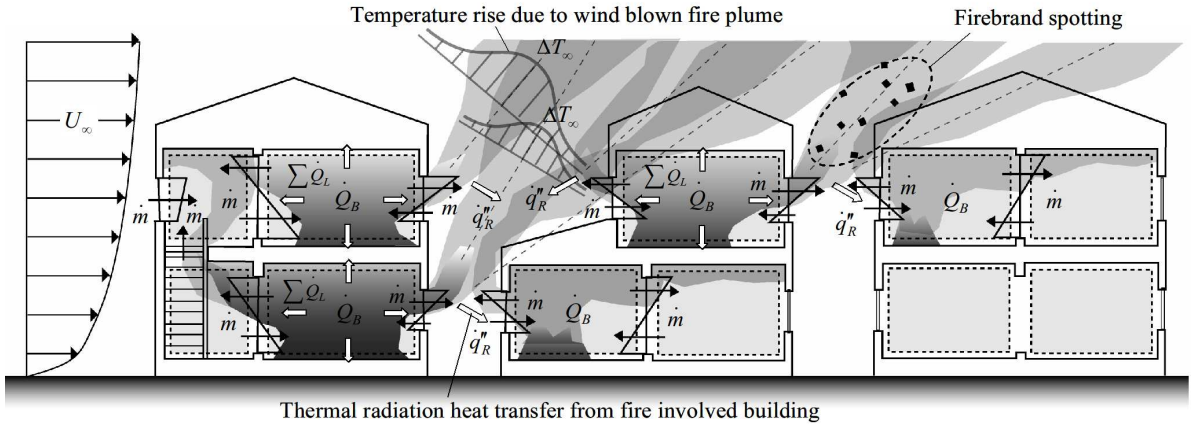

Figure 3.— Schematic of the urban fire spread model.

As to the building fire model, each room of a building is considered as a control volume with uniform physical properties, and transient development of internal fire behaviors are calculated by solving the governing equations for the properties of control volumes simultaneously. Such an approach is generally called zone modeling, which is widely adopted in building fire safety engineering.

As to the building-to-building fire spread, following mechanisms are considered as contributing factors of fire spread:

(I) thermal radiation heat transfer from fire-involved buildings;

(II) thermal convection by wind-blown fire plumes originated from fire-involved buildings in the upwind;

(III) spotting ignition by dispersed firebrands.

Under the influence of the above phenomena, occurrence of fire spread is determined when one of the following conditions is met:

(A) incident heat flux through opening exceeds a critical value $\dot{q}''_{cr}$

(B) surface temperature of exterior wooden wall exceeds a critical value T_{cr}

(C) firebrands at high energy states are fallen upon combustibles.

3 Building fire model

3.1 Governing equations

Following the assumption of the one layer zone model, space occupied by a room inside building is assumed as the control volume in which the properties of gas are uniform. The

conservation equations of mass, energy, and chemical species (the subscripts O and F denote oxygen and gasified fuel, respectively) for an arbitrary control volume is expressed as follows, respectively,

$$\frac{\mathrm{d}}{\mathrm{d}t}\left(\rho_i V_i\right) = \dot{m}_{F,i} - \sum_j \left(\dot{m}_{ij} - \dot{m}_{ji}\right) \tag{1}$$

$$\frac{\mathrm{d}}{\mathrm{d}t}\left(c_P \rho_i T_i V_i\right) = \left(\dot{Q}_{B,i} + c_P \dot{m}_{F,i} T_P\right) - \left\{\sum \dot{Q}_{L,i} + \sum_j \left(c_P \dot{m}_{ij} T_i - c_P \dot{m}_{ji} T_j\right)\right\} \tag{2}$$

$$\frac{\mathrm{d}}{\mathrm{d}t}\left(\rho_i V_i Y_{X,i}\right) = \dot{\Gamma}_{X,i} - \sum_j \left(\dot{m}_{ij} Y_{X,i} - \dot{m}_{ji} Y_{X,j}\right) \tag{3}$$

The state equation of gas is given by,

$$\rho\, T \simeq 353 \tag{4}$$

In the above equations (1–4), c_P is the gas heat capacity, ρ is the gas density, T is the gas temperature, T_P is the pyrolysis temperature of combustible, V is the volume of control volume, Y is the mass fraction of chemical species, $\dot{m}_F$ is the mass production rate of gasified fuel due to pyrolysis of combustibles, $\dot{m}$ is the mass flow rate through opening, $\dot{Q}_B$ is the heat release rate, $\sum \dot{Q}_L$ is the sum of heat loss rate through openings and walls, and $\dot{\Gamma}$ is the mass production rate of chemical species. Subscripts ij and ji denote the direction of mass flow between compartments i and j. Transient change of gas temperature, density, and mass fraction of chemical species are calculated by solving these equations simultaneously.

3.2 Heat release rate inside fire room

In the event of room fire, combustibles stored inside the room receive heat from flame and layer of hot gas accumulated in the upper portion of the room. As a result, the combustibles pyrolyze and produce gasified fuel to sustain fire in the room. It is generally acknowledged that the mass pyrolysis rate of solid material $\dot{m}_F$ can be modeled as a proportional function of the net incident heat flux to the material. However, combustible which is most commonly found in dwellings is wood, and it is not always straightforward to estimate the net incident heat flux since it forms char layer at its irradiated surface. Thus, following experimentally obtained expression is used to calculate mass release rate of the gasified fuel [4],

$$\dot{m}''_F = \begin{cases} 0.86\dot{m}''_0 & (\dot{m}''_0 \leq 0.0082) \\ 0.007 & (0.0082 < \dot{m}''_0 \leq 0.0117) \\ 0.003 + 1.03\dot{m}''_0 \cdot \exp(-94.4\dot{m}''_0) & (0.0117 < \dot{m}''_0) \end{cases} \tag{5}$$

where $\dot{m}''_F$ is the mass pyrolysis rate per unit area, and $\dot{m}''_O$ is the mass inflow rate of oxygen per unit surface area of the combustible.

In the case of ventilation-limited fire, the combustion inside the fire room is restricted by the supply of oxygen. Assuming that the rate of chemical reaction is fast enough, heat release rate inside the fire room is governed by the mass flow rate of oxygen flowing into the fire room,

$$\dot{Q}_{B,O} = \Delta H_O \sum_j (\dot{m}_{ji} Y_{O,j}) \tag{6}$$

where ΔH_O is the amount of heat production when unit mass of oxygen is consumed. While in the case of fuel-lean fire, heat release rate inside the fire room is governed by the mass release rate of gasified fuel,

$$\dot{Q}_{B,F} = \Delta H_F \sum_j (\dot{m}_F + \dot{m}_{ji} Y_{F,j}) \tag{7}$$

where ΔH_F is the heat of combustion of gasified fuel. Considering that the rate of heat release inside the fire room $\dot{Q}_B$ changes continuously at the transition between the ventilation-limited fire and the fuel-lean fire, $\dot{Q}_B$ is given by using the results of equations (6) and (7) as follows,

$$\dot{Q}_B = \min \left\{ \dot{Q}_{B,O}, \dot{Q}_{B,F} \right\} \tag{8}$$

3.3 Mass transfer through openings

When fire starts to generate heat and forms temperature profile inside the fire room, pressure difference δp causes ventilation between the fire room i and the adjacent space j through openings. If the neutral plane of the pressure is between the upper and bottom edges of the opening, mass flow rate in the both directions $\dot{m}_{ij}$ and $\dot{m}_{ji}$ can be calculated by the following equations, respectively,

$$\dot{m}_{ij} = \frac{2}{3} \alpha B \sqrt{2g\rho_i \Delta\rho} \, (H_u - Z_N)^{3/2} \tag{9}$$

$$\dot{m}_{ji} = \frac{2}{3} \alpha B \sqrt{2g\rho_j \Delta\rho} \, (Z_N - H_b)^{3/2} \tag{10}$$

where α is the mass flow rate coefficient, B is the width of the opening, g is the acceleration due to gravity, $\Delta\rho$ is the density difference, H_u is the upper edge height of the opening, H_b is the bottom edge height of the opening, and Z_N is the height of the neutral plane. For pressure inside a room, hydrostatic pressure gradient is assumed,

$$p(z) = p_0 - \rho g \; z + C_W \frac{1}{2} \rho U_\infty^2, \tag{11}$$

where p_0 is the reference pressure of the room relative to the atmospheric pressure at the ground level, C_W is the wind pressure coefficient, and U_∞ is the wind speed. Since the

reference pressure p_0 in Eq. (11) cannot be modeled explicitly, it is implicitly calculated so the resulting mass flow rates $\dot{m}_{ij}$ and $\dot{m}_{ji}$ satisfy the mass conservation Eq. (1). Note that the mass conservation Eq. (1) of a room is not independent from those of other rooms, so the problem is lead to the solution of a system of simultaneous equations.

3.4 Heat Transfer through Openings and Walls

Temperature difference between the fire room and the adjacent room causes heat transfer through compartment boundaries such as openings and walls. This may even cause ignition of combustibles in the adjacent room when intense. As for the heat transfer through opening by thermal radiation compartment gas is assumed as black for simplicity. Thus, the rate of net heat transfer from the space i to the adjacent space j is given by,

$$\dot{Q}_{D,ij} = \left\{\sigma\left(T_i^4 - T_j^4\right) + \dot{q}''_R\right\} A_D \tag{12}$$

where $\dot{q}''_R$ is the radiant heat flux transferred from the neighboring buildings involved in fire, and A_D is the area of the opening.

As for the solid boundaries such as walls and doors, thermal radiation heat transfer and convective heat transfer are considered to give the rate of net heat loss from the compartment gas in room i to the boundary of the adjacent space j as follows,

$$\dot{Q}_{M,ij} = \left\{\varepsilon_M \sigma\left(T_i^4 - T_{M,i}^4\right) + h_M\left(T_i - T_{M,i}\right) + \dot{q}''_R\right\} A_M \tag{13}$$

where ε_M is the emissivity of the boundary surface, h_M is the convective heat transfer coefficient, $T_{M,i}$ is the surface temperature of the boundary, and A_M is the surface area of the boundary. As the thickness of the solid boundary is small compared to the surface area of the exposed surface in general, surface temperature $T_{M,i}$ is calculated by solving the one dimensional heat conduction equation.

4 Building-to-building fire spread model

4.1 Thermal radiation heat transfer from fire involved buildings

Thermal radiation is one of the most important contributing factors which cause building-to-building fire spread. However, extent of its impact is restricted within area relatively close to the building on fire, as radiation from the heat source is shielded by other buildings in densely built urban area. In the model, hot gas inside the fire room and flame ejected from opening are assumed as the two radiation heat sources against the adjacent buildings.

As for the room gas, radiation heat flux transferred from the heat source surface j to another surface of the target building i is expressed as,

$$\dot{q}''_R = \varepsilon \sigma T_j^4 F_{ij}, \tag{14}$$

where ε is the surface emissivity, T is the gas temperature obtained from the governing Eqns. (1–4), σ is the Stefan-Boltzmann constant, and F_{ij} is the view factor.

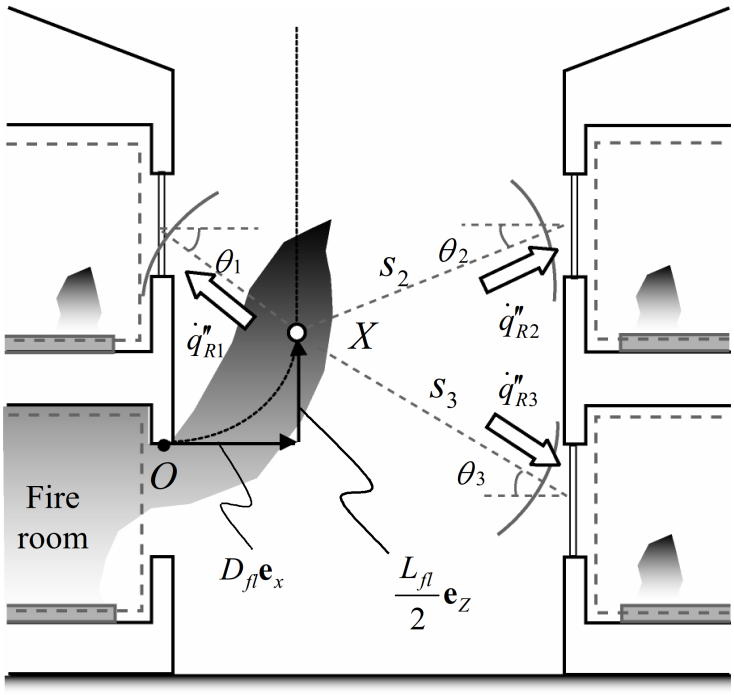

Figure 4.— Thermal radiation heat transfer from an ejected flame.

Schematic diagram of the heat transfer from the window flames is illustrated in Fig. 4. Although the temperature of the window flame varies within its spatial extent, its radiation properties are represented by a point heat source X for simplicity. If the overall heat flux that passes through the surface of a sphere is identical to the overall radiation energy released from the point source, then the radiant heat flux transferred to a building component at the distance of s from the point X will be,

$$\dot{q}''_R = \varepsilon \left(\frac{\chi_R \dot{Q} \cos\theta}{4\pi s^2} \right), \tag{15}$$

where $\dot{Q}$ is the apparent heat release rate of the window flame, χ_R is the fraction of the radiation heat loss to the total heat release, and θ is the angle between the target wall and the line drawn from the point heat source X.

Referring to Fig. 3, position of the point heat source X relative to the reference point O at the upper end of the window is expressed as,

$$\overrightarrow{OX} = D_{fl}\mathbf{e}_X + \frac{L_{fl}}{2}\mathbf{e}_Z, \tag{16}$$

where D_{fl} is the separation between the wall surface and the ejected flame, $\mathbf{e}_X$ is the unit vector normal to the wall, and $\mathbf{e}_Z$ is the unit vector normal to the ground. The separation D_{fl} is calculated with the following equation deduced from the model experiment [5],

$$\frac{D_{fl}}{B} = 0.21F^*, \tag{17}$$

where F^* is the dimensionless parameter defined as follow,

$$F^* \equiv \left(\frac{u_0}{\sqrt{gB}}\right)^2 \left(\frac{\dot{Q}}{\rho_\infty c_P T_\infty B\left(H - Z_N\right)^{3/2}}\right)^{-2/3}, \tag{18}$$

where u_0 is the maximum horizontal flow velocity at the opening, $\dot{Q}$ is the apparent heat release rate, T_∞ is the ambient temperature, and ρ_∞ is the ambient density. Equations (17) and (18) show that the separation D_{fl} gets larger when either the horizontal velocity u_0 gets larger or the apparent heat release rate $\dot{Q}$ gets smaller. On the other hand, the flame height L_{fl} is assumed as the height of the boundary between the intermittent flame region and the plume region as follows [6],

$$\frac{L_{fl}}{H - Z_N} = 2.44, \tag{19}$$

Although the flame height L_{fl} in Eq. (19) is independent from the heat release rate $\dot{Q}$, it implicitly incorporates the effect of $\dot{Q}$ by introducing the height of the venting surface $H - Z_N$.

4.2 Thermal Convection by The Wind-blown Fire Plumes

Wind-blown fire plume envelopes area in the downwind of the fire involved building and elevates ambient temperature enhancing ignitability of combustibles (Fig. 4). Although the nature of wind-blown fire plume is complex, it is assumed that the temperature rise along the trajectory ΔT_m can be approximated by that of a point heat source in a quiescent atmosphere [7],

$$\Delta T_m = 24\left(\frac{\xi}{\dot{Q}^{2/5}}\right)^{-5/3}, \tag{20}$$

where ξ is the length along the plume trajectory. Radial distribution from the trajectory is the normal distribution, that is,

$$\frac{\Delta T(r)}{\Delta T_m} = \exp(-(r/b_T)^2), \tag{21}$$

where r is the radial distance, and b_T is the half-width of the temperature rise. Another assumption is that the wind is strong enough when fire spread takes place, so that the power-law wind profile is unaffected by the fire plume.

In order to evaluate temperature elevation around a building in the downwind from Eq. (21), the distance from the trajectory to the target building r is needed. For this, the inclined angle θ of the fire plume trajectory is given by the following expression [8],

$$\tan\theta = 0.1\Omega^{-3/4}, \tag{22}$$

where Ω is the dimensionless wind velocity defined as follows,

$$\Omega \equiv \frac{U_\infty}{\left(\dfrac{\dot{Q}' g}{c_p \rho_\infty T_\infty}\right)^{1/3}}, \tag{23}$$

where U_∞ is the wind velocity, $\dot{Q}'$ is the heat release rate per unit length calculated as $\dot{Q}' = \dot{Q}/\sqrt{A_{floor}}$, and A_{floor} is the floor area.

4.3 Spotting ignition by dispersed firebrands

Among the enormous number of firebrands released into the fire-induced flow field, it is only a fraction of them which actually cause fire spread. The occurrence of spotting ignition by a firebrand depends upon several conditions, such as, the properties of the firebrand, properties of the target combustible, local-scale wind conditions, atmospheric conditions, etc.. However, since the mechanism of firebrand ignition is not well studied, the occurrence of the fire spread caused by the i-th firebrand at a building with the relative spatial coordinate (X, Y) is modeled as proportional to the distribution probability of transported firebrand $p_{B,i}$. The distribution probability $p_{B,i}$ is described by incorporating the results of the numerical simulation on the transport behaviors of disk-shaped firebrands [9]. Setting the coordinate origin O' at the fire involved building, scattering probability of firebrands along the wind direction (that is, X-axis) is approximated by the log-normal distribution $p_{B,X}$, and that of the orthogonal direction (that is, Y-axis) is approximated by the normal distribution $p_{B,i}$. With these, the overall distribution is given as a product of $p_{B,X}$ and $p_{B,Y}$, which is,

$$p_B = p_{B,X} \cdot p_{B,Y}, \tag{24}$$

$$\begin{cases} p_{B,X} = \dfrac{1}{\sqrt{2\pi}\sigma_{L,X} X} \exp\left(-\dfrac{\left(\ln X - \mu_{L,X}\right)^2}{2\sigma_{L,X}^2}\right), \quad (0 < X < \infty), \\ p_{B,Y} = \dfrac{1}{\sqrt{2\pi}\sigma_Y} \exp\left(-\dfrac{Y^2}{2\sigma_Y^2}\right), \quad (0 < Y < \infty), \end{cases}$$

where $\mu_{L,X}$ and $\sigma_{L,X}$ are the mean and standard deviation of logarithm natural of the transport distance $\ln X$, respectively. Whereas for the orthogonal direction to the wind (Y-direction), the mean transport distance is zero, and only its standard deviation σ_Y is considered.

The scattering distribution of firebrands is evaluated by substituting $\mu_{L,X}$, $\sigma_{L,X}$ and σ_Y into the Eq. (24), which are [9],

$$\frac{\mu_X}{D} = 0.47\left(B^*\right)^{2/3} \text{ and } \frac{\sigma_X}{D} = 0.88\left(B^*\right)^{1/3}, \tag{25}$$

$$\frac{\mu_Y}{D} = 0 \text{ and } \frac{\sigma_Y}{D} = 0.0.92, \tag{26}$$

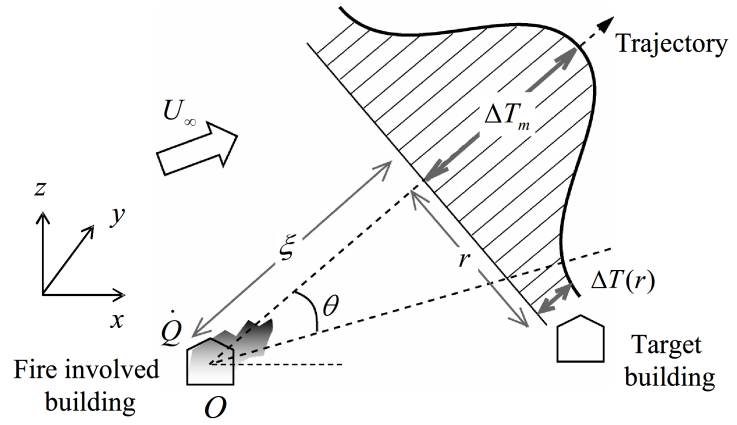

Figure 5.— Temperature rise due to a wind-blown fire plume.

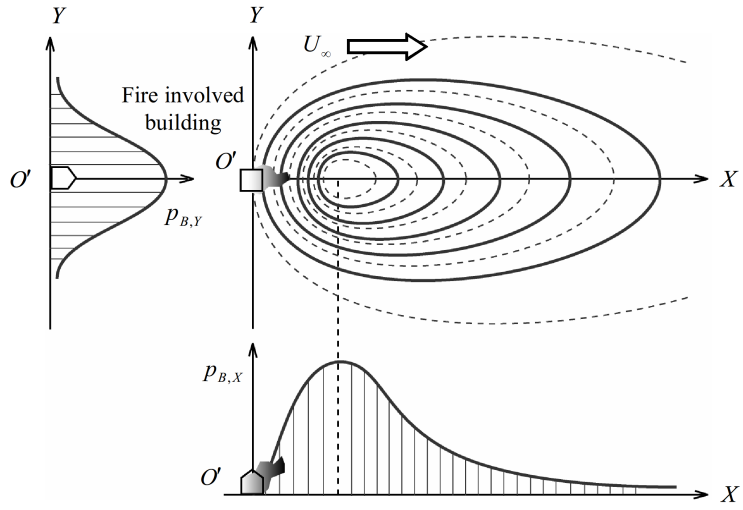

Figure 6.— Probability of firebrand scattering released from a fire involved building.

Note that μ_X and σ_X need to be converted into the form of logarithm natural, that is $\mu_{L,X}$ and $\sigma_{L,X}$, before substituting into Eqs. (25) and (26). The dimensionless parameter B^*, which governs the transport behaviors of firebrands, is a combined function of the dimensionless wind speed $U_\infty/\sqrt{gD}$, dimensionless density ρ_P/ρ_∞, dimensionless length d_P/D, and dimensionless heat release rate $\dot{Q}/\left(\rho_\infty c_P T_\infty g^{1/2} D^{5/2}\right)$, as follows,

$$B^* \equiv \frac{U_\infty}{\sqrt{gD}} \left(\frac{\rho_P \, d_P}{\rho_\infty D} \right)^{-3/4} \left(\frac{\dot{Q}}{\rho_\infty c_P T_\infty g^{1/2} D^{5/2}} \right)^{1/2}, \tag{27}$$

where D is the length scale of the fire origin, which is calculated as a square root of the floor area $\sqrt{A_{floor}}$, ρ_P is the firebrand density, and d_P is the width of the square shaped firebrand.

5 Fire spread risk assessment of Kyoto Higashiyama area

The presented model was applied to Kyoto Higashiyama area and the risk of fire spread was analyzed. The area is well known as one of the representatives of the densely-built urban areas, as well as those of Japanese traditional city areas which contain several historical monuments.

Figure 7.— Aerial view of Kyoto Higashiyama area [10].

The aerial view of the target city area is shown in Fig. 7. There is a low range of hills (Higashiyama Mountains) on the east side, so the majority of the area is sited on a slight slope. While on the west side, there is a river (Kamogawa River) about 60m wide flowing from north to south. As shown in Fig. 8, traditional Japanese houses generally have exposed wooden members on their façades. Although the sequence of the wooden fa¸çades is one of the principal factors of traditional cityscape, they have risk of getting damage from fires in adjacent buildings. Improvement of fire safety in densely-built areas of historical cities has particular importance in preserving the unique culture of cities. The assessment of fire spread risk in such city areas will provide guidance to the design of effective countermeasures.

5.1 Fire spread simulation in Kyoto Higashiyama area

In order to verify the basic characteristics of the presented fire spread model and the general behavior of fire spread in the target urban area, a fire spread simulation was carried out. The computational domain is a rectangular area which covers 2.0km in the west-east and 1.5km in the north-south directions (Fig. 7). Information needed for the fire spread simulation, such as building configuration, building construction type, or topography were

Figure 8.— Cityscape in Kyoto Higashiyama area.

produced from the GIS data, city planning maps and aerial survey photographs. The area involves 7909 buildings in total, and 6505 of them (i.e., 82.2 %) were wood-frame constructions. The standard weather data, obtained from the Automated Meteorological Data Acquisition System (AMeDAS) from 1981 to 1995, was used as the input weather data on ambient temperature and wind velocity/direction.

The result of the fire spread simulation is illustrated in Fig. 10. The arrow in the center of the computational domain indicates the fire origin. Polygons in red and black correspond to burning buildings and burnt out buildings, respectively. The fire spread almost concentrically around the fire origin in the early stages. However, Fig. 10 shows that the fire had jumped over Higashioji Street (about 15m wide) by 5 hrs after the outbreak. The wind direction was generally from the west to the east throughout the computation. Thus, one important reason for the jump is attributed to firebrands causing distant ignitions in the leeward area. By 10 hrs after the outbreak, the fire front reached as far as the city boundary at the foot of Higashiyama Mountain in the east. Whereas, the fire front in the west side almost reached Kamogawa river (about 60m wide). The rate of fire spread was faster in the east, because buildings in the leeward side of the burning area were exposed to wind-blown fire plumes. The wind velocity was higher than usual in Kyoto city, i.e., the average velocity throughout the computation was 3.5m/s. However, in the later stage of the computation, the spread of fire in the north and south directions was stopped by open spaces including wide streets. The eventual number of burnt out buildings in the Higashiyama area was around 2000. The number of burnt out buildings in the 1976 Sakata Fire, which lasted about 11 hrs, was 1744. Although the conditions affecting fire spread are distinct, the sizes of these fires were similar.

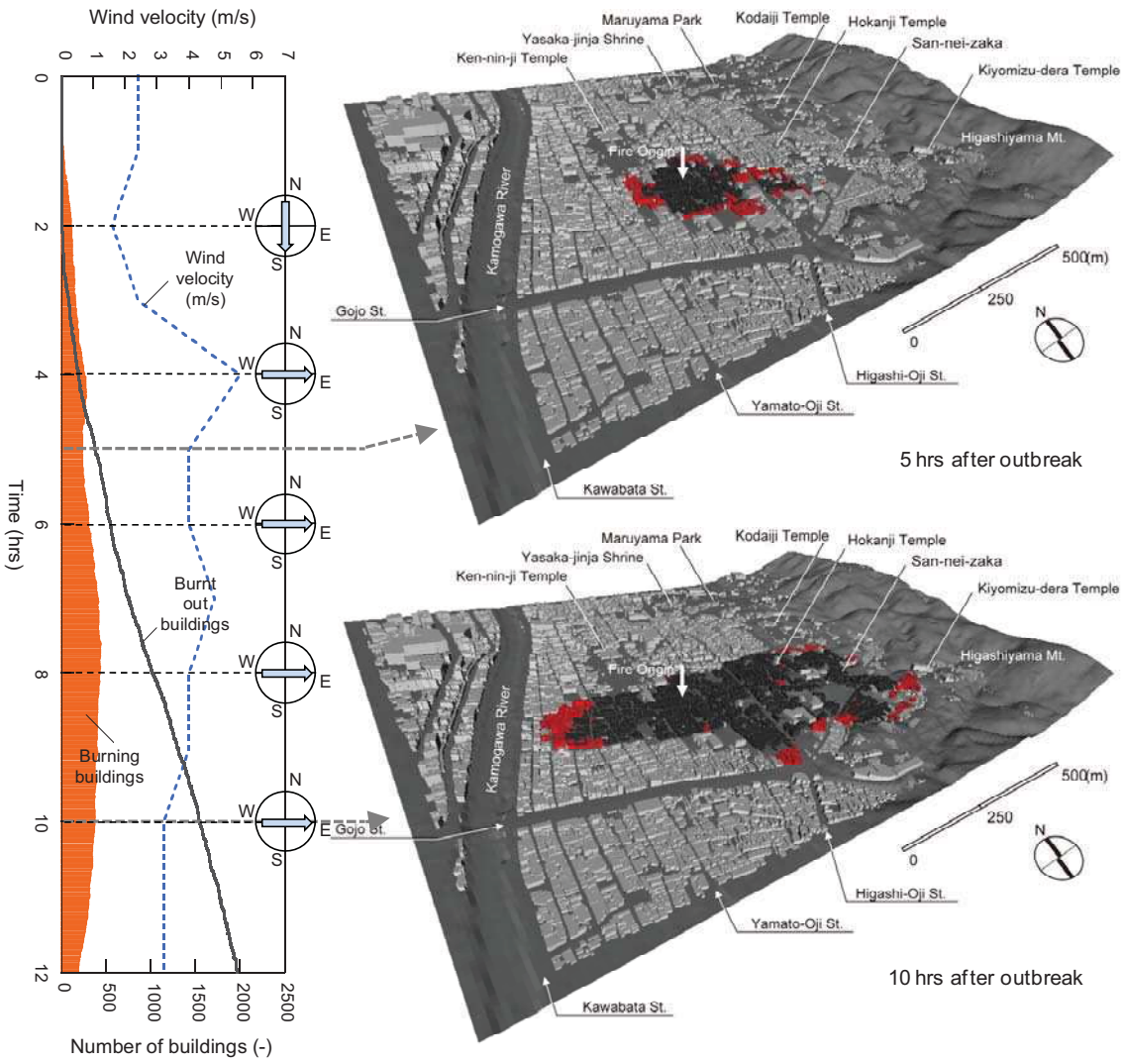

Figure 9.— An example of the fire spread simulation.

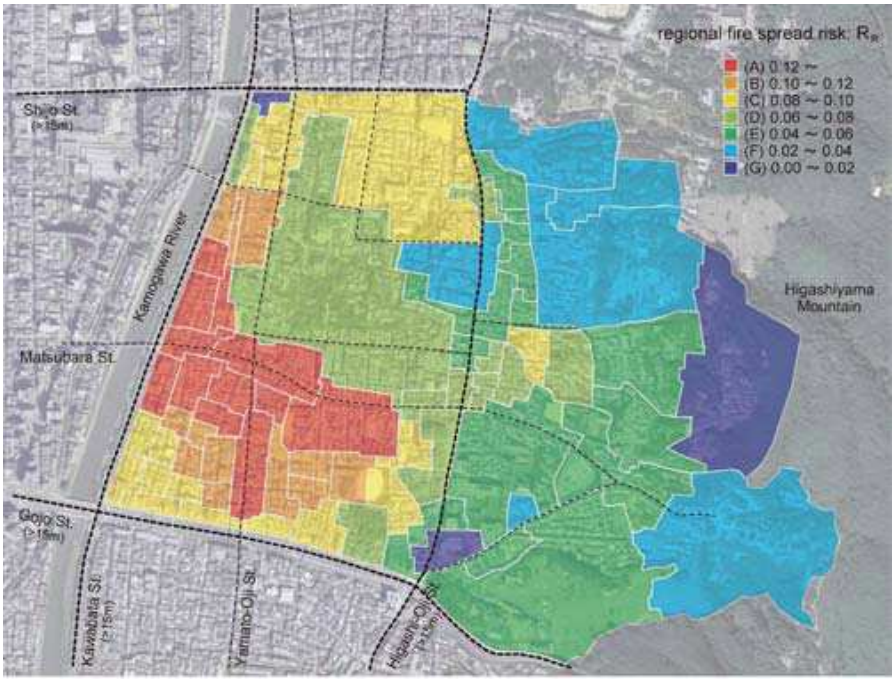

Figure 10.— Estimated fire spread risk in Kyoto Higashiyama area (present).

5.2 Fire spread risk assessment and evaluation of a fire safety measure

The result of fire spread simulation shown in Fig. 9 is not representing the general fire spread risk of the target area, but it is only a case result under a certain ignition and weather condition. The risk of fire spread can be evaluated by the Monte Carlo Simulation, which estimates the expectation value of loss due to fire spread. The regional risk of fire spread R_R is deduced by consolidating result of the Monte Carlo Simulation as follows,

$$R_R \equiv \frac{\sum_{i=1}^{N} (p_{R,i} L_{R,i})}{n_R}, \tag{28}$$

where p_B is the probability of a building to catch on fire out of all the expected fire scenarios, L_B is the number of burnt out buildings, and n_R is the number of buildings in the area. The fire spread risk R_R is congruent to the average probability of fire for a group of buildings.

The parameters which were varied probabilistically in order to carry out the Monte Carlo Simulation in this study were the outbreak conditions (ignition point and time) and weather conditions (ambient temperature, direction and velocity of wind). The time of fire outbreak was given randomly regardless of building construction or the use of appliances.

The target city area consists of multiple administrative units. The regional risks of fire spread R_R for the individual administrative unit is color-coded in Fig. 10. The results for the units near the computational boundary are omitted, because the effect of fire spread from the adjacent units is not adequately evaluated in such areas. Regional

risk is the highest in the south-western part of the area, and it is comparatively low in the eastern part. In general, regional risk is high in areas at high building coverage and high wooden building ratios. Similarly, regional risk of areas along broad streets (>15m) is rated relatively low, as fire spread from the other side of the street seldom takes place. However, as the eastern part of the area has Higashiyama Mountains on one side, evacuation routes for residents will be restricted in case of urban conflagration starting in the western area. In other words, the regional fire spread risk in Fig. 10 is not congruent with the risk of evacuation.

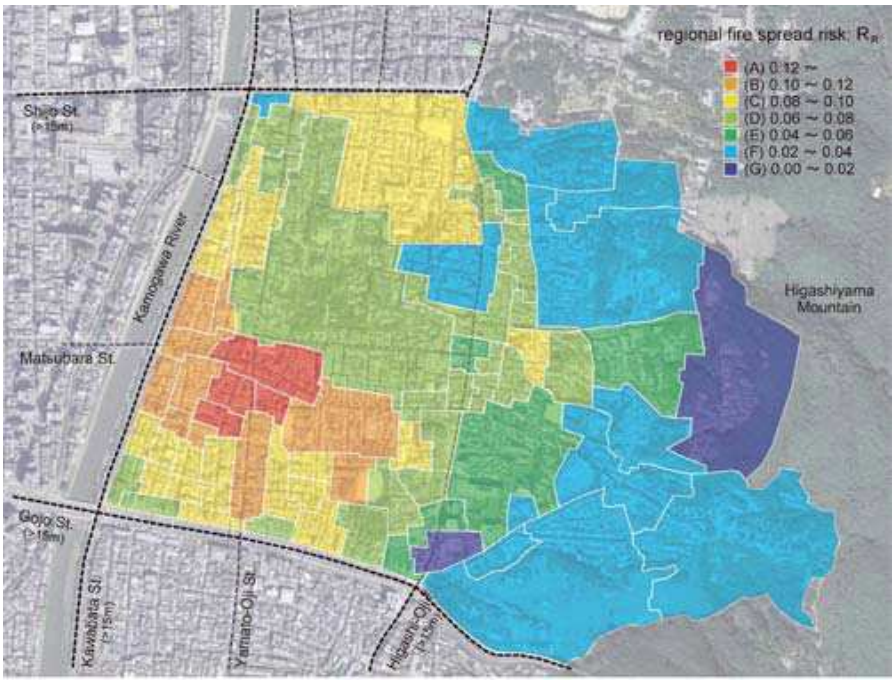

Figure 11.— Estimated fire spread risk in Kyoto Higashiyama area (if the fire safety measure was implemented).

Effectiveness of a fire safety measure can be evaluated by comparing the regional fire spread risk R_R before and after its implementation. As a case study, effectiveness of reinforcement of exterior walls on reduction of the fire spread risk R_R was investigated. Among all the wood-frame buildings in the target city area, 50% of them were assumed to be reinforced. Due to the reinforcement, the burn-through time (an index of fire resistant performance for a wall) was assumed to be extended from 20min to 40min. The estimated result is shown in Fig. 11. As buildings became more fire-resistant individually, the risk R_R was reduced especially in the south-western area. However, the effectiveness of the fire safety measure was limited, that there are still a number of administrative units of high fire spread risk left within the target city area. Although the reinforcement of exterior walls was effective in reducing the rate of fire spread in the target area, occurrence of fire spread itself was not prevented. In the present simulation, the effect of fire fighting activity by

firefighters or residents was not considered. However, firefighting activity would operate most efficiently when the rate of fire spread was reduced by the reinforcement of exterior walls. Thus, the reduction rate of the fire spread risk R_R would be more evident in fire scenarios with firefighting activity.

6 Conclusions

In this paper, framework of a physics-based model for urban fire spread was presented. The model is applicable to the evaluation of fire spread risk in densely-built urban areas, as it is capable of evaluating the loss in a quantitative way. As a case study, risk and behavior of fire spread in Kyoto Higashiyama area was analyzed. Effectiveness of a fire safety measure was evaluated by comparing the estimated fire spread risk of the target city area before and after its implementation.

References

[1] Japan Association for Fire Science and Technology, Report of The Fire Damage caused by The 1995 Kobe Earthquake, 1996 (in Japanese).

[2] Ministry of Land, Infrastructure and Transport, Disaster Resilient City Planning for Urban Regeneration, 2003 (in Japanese).

[3] Himoto K, Tanaka T. Development and Validation of A Physics-based Urban Fire Spread Model, Fire Safety Journal, Vol. 43, No. 7, pp. 477–494, 2008.

[4] Ohmiya Y, Tanaka T, Wakamatsu T. Burning Rate of Fuels and Generation Limit of the External Flames in Compartment Fire, Fire Science and Technology, Vol. 16, No. 1/2, pp. 1–12, 1996.

[5] Himoto K, Tsuchihashi T, Tanaka Y, TanakaT. Modeling Thermal Behaviors of Window Flame Ejected from a Fire Compartment. Fire Safety Journal, Vol. 44, No. 2, pp. 230–240, 2009.

[6] Himoto K, Tsuchihashi T, Tanaka Y, TanakaT. Modeling the Trajectory of Window Flames with Regard to Flow Attachment to the Adjacent Wall. Fire Safety Journal, Vol. 44, No. 2, pp. 250–258, 2009.

[7] Beyler CL. Fire Plumes and Ceiling Jets. Fire Safety Journal, Vol. 11, pp. 53–75, 1986.

[8] Yokoi S. Temperature Distribution in The Downwind of A Line Fire, Disaster Research, Non-life Insurance Rating Organization of Japan, Vol. 7, pp. 151–159, 1970 (in Japanese).

[9] Himoto K, Tanaka T, Transport of Disk-shaped Firebrand in A Turbulent Boundary Layer, Proceedings 8th Symposium, International Association for Fire Safety Science, pp. 433–444, 2005.

[10] Live search maps (http://maps.live.com/)